Progress In Electromagnetics Research, PIER 72, 145–158, 2007

ANGULAR-DIVERSITY RADAR RECOGNITION OF SHIPS BY TRANSFORMATION BASED APPROACHES — INCLUDING NOISE EFFECTS

K.-C. Lee, J.-S. Ou, and C.-W. Huang

Department of Systems and Naval Mechatronic Engineering
National Cheng-Kung University
Tainan 701, Taiwan

Abstract—In this paper, the angular-diversity radar recognition of ships is given by transformation based approaches with noise effects taken into consideration. The ships and sea roughness are considered by simplified models in the simulation. The goal is to identify the similarity between the unknown target ship and known ships. Initially, the angular-diversity radar cross sections (RCS) from a ship are collected to constitute RCS vectors (usually large-dimensional). These RCS vectors are projected into the eigenspace (usually small-dimensional) and radar recognition is then performed on the eigenspace. Numerical examples show that high recognition rate can be obtained by the proposed schemes. The radar recognition of ships in this study is straightforward and efficient. Therefore, it can be applied to many other radar applications.

1. INTRODUCTION

Radar recognition of ships plays an important role in coast guard control, sea rescue, regulation of shipping channels and naval warfare. In the radar recognition of ships, many existing studies utilize different approaches to recognize the ship targets by their SAR or ISAR images, e.g., [1, 2]. This motivates us to develop an alternative approach for the radar recognition of ships.

In this paper, the angular-diversity radar recognition of ships is given by transformation based approaches with noise effects taken into consideration. The ships and sea roughness are considered by simplified models in the simulation. The goal is to identify the similarity between the unknown target ship and known ships. The idea of angular-diversity comes from microwave diversity imaging

[3, 4]. Initially, the angular-diversity radar cross sections (RCS) from a ship are collected to constitute RCS vectors (usually large-dimensional). By changing the elevation angle or the ship type, different RCS vectors are obtained to produce a high-rank covariance matrix. The eigenvalues and eigenvectors of the covariance matrix are solved by the Karhunen-Loève's low-rank approximation [5]. By choosing some of the largest eigenvalues and their corresponding eigenvectors, all the RCS vectors are projected into the eigenspace (usually small-dimensional). Similarity between the unknown target ship and known ships can be identified in the eigenspace with high recognition rate. This will reduce the complexity for radar recognition of RCS characteristics from ships.

The above transformation mainly comes from the principal components analysis (PCA) [6, 7]. The PCA is usually exploited in the fields of digital imaging processing and pattern analysis. In those fields, the training or testing data of PCA usually represent shapes of object images. However, the training or testing data of PCA in this study are the RCS characteristics from ships. To our knowledge, this is the first study to combine the RCS and PCA in radar recognition of ships. The radar recognition of ships is performed on the eigenspace. Numerical examples show that high recognition rate can be obtained by the proposed schemes. The radar recognition of ships in this study is straightforward and efficient. Therefore, it can be applied to many other radar applications.

In Section 2, the theoretical formulations are given. Numerical simulation results are given in Section 3. Finally, the conclusion is given in Section 4.

2. FORMULATIONS

Consider a ship on the sea level (X-Y plane) located at the origin of coordinate, as shown in Figure 1. The front end of ship is in the $+\hat{x}$ direction and the broadside of ship is in the $\pm\hat{y}$ direction. The spherical coordinate system is defined as (R, θ, ϕ) where R is the distance from observation position to origin, θ is the elevation angle and ϕ is the azimuth angle. The ship is illuminated by a plane wave $\overline{E}_i = e^{+jkx}\hat{z}$ where k is the wavenumber. The bistatic RCS in the direction of (θ, ϕ) is defined as

$$\sigma(\theta, \phi) = \lim_{R\to\infty} 4\pi R^2 \frac{\left|\overline{E}_s(\theta, \phi)\right|^2}{\left|\overline{E}_i\right|^2}. \tag{1}$$

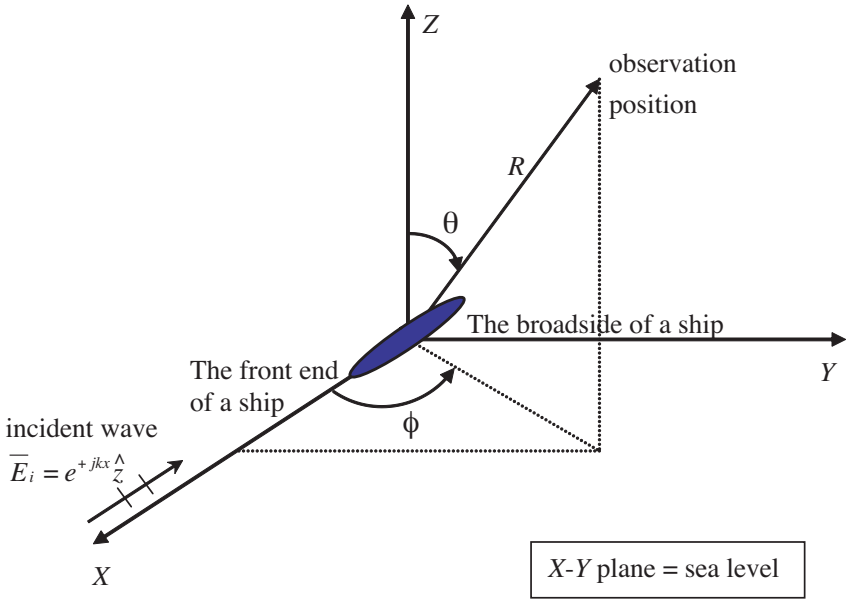

Figure 1. Schematic diagram of a ship illuminated by an incident plane wave.

where $\overline{E}_s(\theta, \phi)$ is the scattered electric field. The bistatic RCS of a ship at a fixed elevation angle θ and different azimuth angles of ϕ are collected to constitute an RCS vector. Different RCS vectors are collected and processed by the transformation based approaches. The flow chart of the transformation based angular-diversity RCS radar recognition scheme is shown in Figure 2. Each step in Figure 2 is interpreted in detail as the following.

Step-1: Select training vectors

Assume we have P types of known ships and $p = 1, 2, \ldots, P$ denote the types of ships. As mentioned above, an RCS vector represents the bistatic RCS for a type of known ship at a fixed elevation angle θ and N different azimuth angles of ϕ. This RCS vector is N-dimensional. By choosing M_p elevation angles for the p-th type of ship, M_p RCS vectors are obtained to constitute the p-th class of RCS characteristics. Therefore, we have $M = \sum_{p=1}^{P} M_p$ RCS vectors for all the P types of known ships. These M RCS vectors are denoted as $\overline{X}_i$, $i = 1, \ldots, M$ and serve as the training vectors of our recognition algorithm.

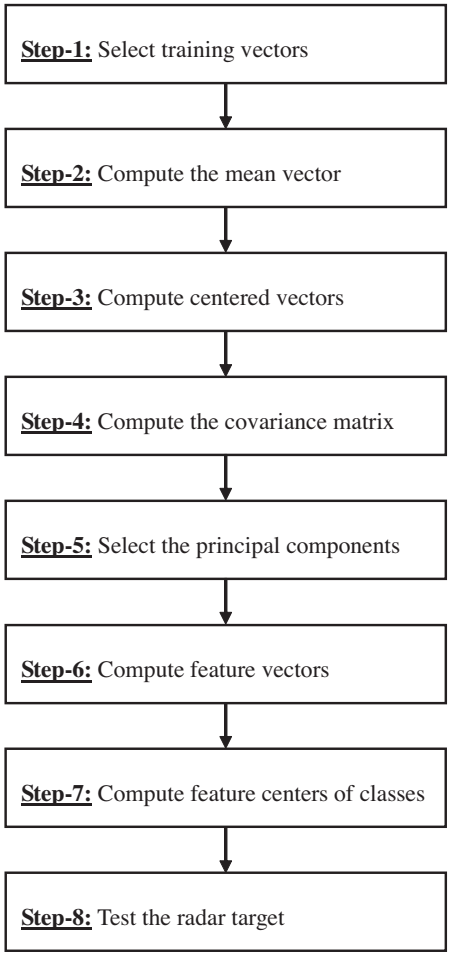

Figure 2. Flow chart of the transformation based radar recognition scheme.

Step-2: Compute the mean vector

The mean vector $\overline{\Psi}$ of the M training vectors in Step-1 is given as

$$\overline{\Psi} = \frac{1}{M} \sum_{i=1}^{M} \overline{X}_i. \tag{2}$$

Step-3: Compute centered vectors

Transform the RCS vectors into centered vectors. The centered

vector $\overline{\Phi}_i$ for an N-dimensional RCS vector $\overline{X}_i$ in Step-1 is given as

$$\overline{\Phi}_i = \overline{X}_i - \overline{\Psi}, \quad i = 1, \ldots, M \tag{3}$$

Obviously, every centered vector is also N-dimensional.

Step-4: Compute the covariance matrix

The covariance matrix $\overline{\overline{C}}$ is defined as

$$\overline{\overline{C}} = \frac{1}{M} \overline{\overline{A}} \cdot \overline{\overline{A}}^T \tag{4}$$

where

$$\overline{\overline{A}} = \left(\overline{\Phi}_1, \quad \overline{\Phi}_2, \quad \cdots, \quad \overline{\Phi}_M \right) \tag{5}$$

and "T" denotes the transpose. The dimension of $\overline{\overline{A}}$ is $N \times M$ and thus the dimension of $\overline{\overline{C}}$ is $N \times N$.

The dimension N represents the number of angular diversity in collecting RCS of a ship and is large in general. Therefore, the computation for eigenvalues and eigenvectors of the $N \times N$ covariance matrix $\overline{\overline{C}}$ is inefficient due to the large dimension of matrix. Since only the principal eigenvalues and eigenvectors are required in our recognition procedures, the Karhunen-Loève's low-rank approximation [5] is utilized and is described in the following.

Consider the $M \times M$ matrix $\overline{\overline{L}}$ defined as

$$\overline{\overline{L}} = \frac{1}{M} \overline{\overline{A}}^T \cdot \overline{\overline{A}} \tag{6}$$

Note that we have $M \ll N$ in general. The eigenvalues and eigenvectors of $\overline{\overline{L}}$ are easy to obtain. Assume that λ_i and $\overline{v}_i$, $i = 1, \ldots, M$ are the eigenvalues and eigenvectors of the $M \times M$ matrix $\overline{\overline{L}}$. In linear algebra, one can easily prove that λ_i and $\overline{\overline{A}} \cdot \overline{v}_i$, i=1,..., M are the eigenvalues and eigenvectors of the $N \times N$ matrix $\overline{\overline{C}}$. In other words, the principal eigenvalues and eigenvectors of the $N \times N$ matrix $\overline{\overline{C}}$ can be obtained by solving the eigenvalues and eigenvectors of the $M \times M$ matrix $\overline{\overline{L}}$.

Step-5: Select the principal components

We select the M' largest eigenvalues ($M' < M$) and the corresponding eigenvectors of $\overline{\overline{C}}$. The eigenvectors are normalized as

$$\overline{u}_i = \overline{\overline{A}} \cdot \overline{v}_i \Big/ \left| \overline{\overline{A}} \cdot \overline{v}_i \right| \quad , i = 1, \ldots, M'. \tag{7}$$

The M' eigenvalues and their corresponding eigenvectors serve as the principal components in our radar recognition of ships.

Step-6: Compute feature vectors

For an N-dimensional RCS vector $\overline{X}$, it can be projected into an M'-dimensional eigenspace spanned by vector bases of (7). The projection result is an M'-dimensional feature vector $\overline{\Omega}$ given as

$$\overline{\Omega} = [\omega_1 \quad \omega_2 \quad \cdots \quad \omega_{M'}]^T \tag{8}$$

where

$$\omega_i = \overline{u}_i^T \cdot \left(\overline{X} - \overline{\Psi}\right), \quad i = 1, \ldots, M'. \tag{9}$$

The goal of this step is to reduce the dimension of RCS vectors so that the radar recognition of ships can be easy and efficient.

Step-7: Compute the feature centers of classes

For the p-th class, the M_p RCS vectors are projected into the M'-dimensional eigenspace and then M_p feature vectors are obtained. The feature center $\overline{\Omega}_p^{mean}$ of the p-th class is defined as the mean vector of these M_p feature vectors. All the P classes of training vectors in Step-1 are treated and then P feature centers of classes are obtained totally.

Step-8: Test the radar target

For an unknown target ship, its angular-diversity RCS at a fixed elevation angle θ and different N azimuth angles of ϕ are collected to constitute an RCS vector $\overline{X}$. This RCS vector $\overline{X}$ is N-dimensional and is projected into the M'-dimensional eigenspace according to (8) and (9) to produce a feature vector $\overline{\Omega}$. The distance, i.e., class error, of this measurement with respect to the p-th class is given by

$$d_p = \left|\overline{\Omega} - \overline{\Omega}_p\right|, \quad p = 1, \ldots, P. \tag{10}$$

The magnitude of distance (class error) in (10) is in inverse proportion to the degree of similarity. The smallest distance (class error) means that the target ship has the highest degree of similarity with the corresponding type of ship.

3. NUMERICAL SIMULATION RESULTS

In this section, numerical examples are given to illustrate the above formulations. To easily obtain the scattering data, simplified ship models for simulation are utilized instead of real ships. Assume there

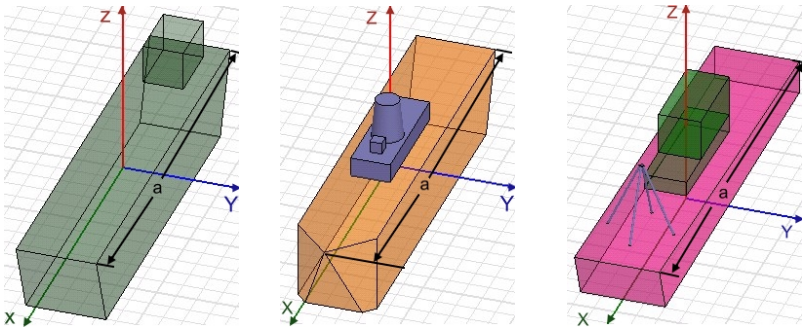

(a) (b) (c)

Figure 3. Geometrical models for three known classes of ships: (a) type I, (b) type II and (c) type III.

are three types of known ships ($P = 3$) including type I (similar to container vessel), type II (similar to naval ship) and type III (similar to fishing boat). The geometrical models for the three types of known ships are shown in Figure 3. The ship length a is chosen to be $ka = 9.4$ for the ship of type I, $ka = 6.3$ for the ship of type II, and $ka = 3.1$ for the ship of type III. All ships are in rough sea waters (X-Y plane). The characteristic for surface roughness of sea water is assumed to be

$$z(x, y) = \frac{4}{75}a \cdot \sin\left(\frac{15\pi}{4}x\right) \sin\left(\frac{15\pi}{4}y\right) + \frac{8}{75}a. \tag{11}$$

The sea water has dielectric constant $\varepsilon_r = 81$ and conductivity $\sigma = 4\,\mathrm{S/m}$. As the arrangement in Figure 1, the bistatic RCS from each type of known ship at a fixed elevation angle θ and 181 azimuth angles of $\phi = 0°, 1°, \ldots, 180°$ are collected to constitute an RCS vector, i.e., $N = 181$. The training vectors of RCS for each type of known ship are obtained by sampling the elevation angles at $\theta = 61°$, $63°$,..., $89°$. Therefore, we have $M_1 = M_2 = M_3 = 15$ and $M = 45$. The number of principal components is chosen to be $M' = 2$.

In the simulation of RCS, the commercial software Ansoft HFSS is exploited. Initially, the bistatic RCS from a perfectly conducting sphere centered at the coordinate origin is simulated by the Ansoft HFSS. The dimension of the perfectly conducting sphere is chosen to be $ka_0 = 1.1$ or $ka_0 = 7.7$ (a_0 is the sphere radius) so that the results of RCS by Ansoft HFSS software and those of [8] can be compared under the same condition. It is found that the results of RCS by our simulation of Ansoft HFSS are consistent with those given in [8]. The purpose of this process is to verify that our operation of Ansoft

HFSS software is correct. After our software operation is verified to be correct, the RCS from ships are simulated by the Ansoft HFSS.

The radar recognition algorithm is trained using Step-1 to Step-7 in Figure 2 or Section 2. After the algorithm is well trained, it can identify the unknown target of ship by using Step-8 in Figure 2 or Section 2. In the testing, there are three examples to verify the identification of the algorithm.

In the first example, the testing target ship is the ship of type I. The RCS is collected at a specified elevation angle within the range of $60^\circ \leq \theta \leq 90^\circ$ and this elevation angle is different from those of the training data in Step-1. The RCS is collected at this elevation angle and at azimuth angles of $\phi = 0^\circ, 1^\circ, \ldots, 180^\circ$ to constitute a testing RCS vector $\overline{X}$. Following the Step-8 given in Figure 2 or Section 2, the testing for radar recognition of ships is performed. Figure 4 shows the distance (class error) to feature centers for the three known classes of ship RCS under 15 testing elevation angles at $\theta = 62^\circ, 64^\circ, \ldots, 90^\circ$.

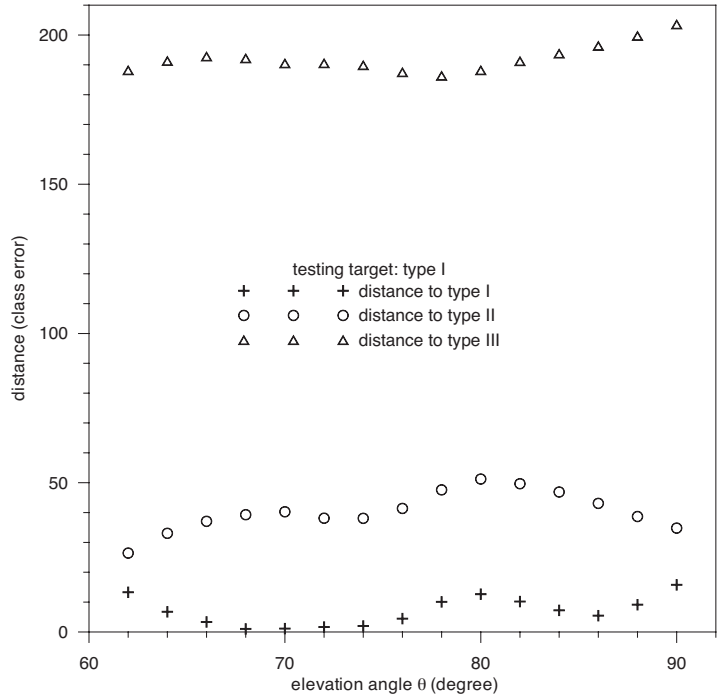

Figure 4. The distance (class error) to feature centers for the three known classes of ship RCS at different elevation angles θ by using ship of type I as the testing target.

It should be emphasized that these testing elevation angles are not included in the training data of Step-1. From Figure 4, it is found that the smallest distance (class error) at every testing elevation angle is just the distance to class of type I. In other words, of all the three types of known ships, the ship of type I resembles unknown target most. This result is very reasonable and the successful recognition rate is 100% (=15/15).

In the second example, the testing target ship is the ship of type II. The radar recognition procedures are the same as those given in the first example. Figure 5 shows the distance (class error) to feature centers for the three known classes of ship RCS under 15 testing elevation angles at $\theta = 62^\circ, 64^\circ, \ldots, 90^\circ$. From Figure 5, it is found that the smallest distance (class error) at 15 testing elevation angles is the distance to class of type II. In other words, of all the three types of known ships, the ship of type II resembles unknown target most. This result is very reasonable and the successful recognition rate is 100% (=15/15).

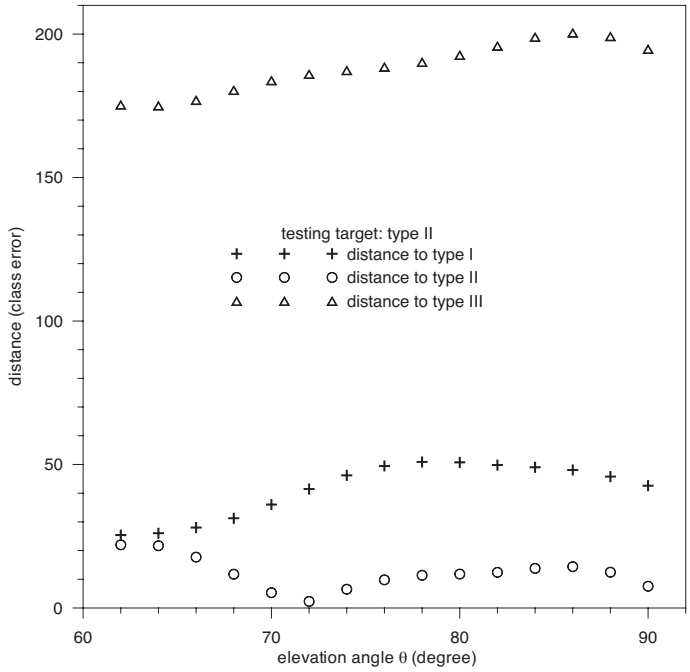

Figure 5. The distance (class error) to feature centers for the three known classes of ship RCS at different elevation angles θ by using ship of type II as the testing target.

In the third example, the testing target ship is the ship of type III. The radar recognition procedures are the same as those given in the first example. Figure 6 shows the distance (class error) to feature centers for the three known classes of ship RCS under 15 testing elevation angles at $\theta = 62^\circ, 64^\circ, \ldots, 90^\circ$. From Figure 6, it is found that the smallest distance (class error) at every testing elevation angle is just the distance to class of type III. In other words, of all the three types of known ships, the ship of type III resembles unknown target most. This result is very reasonable and the successful recognition rate is 100% (=15/15).

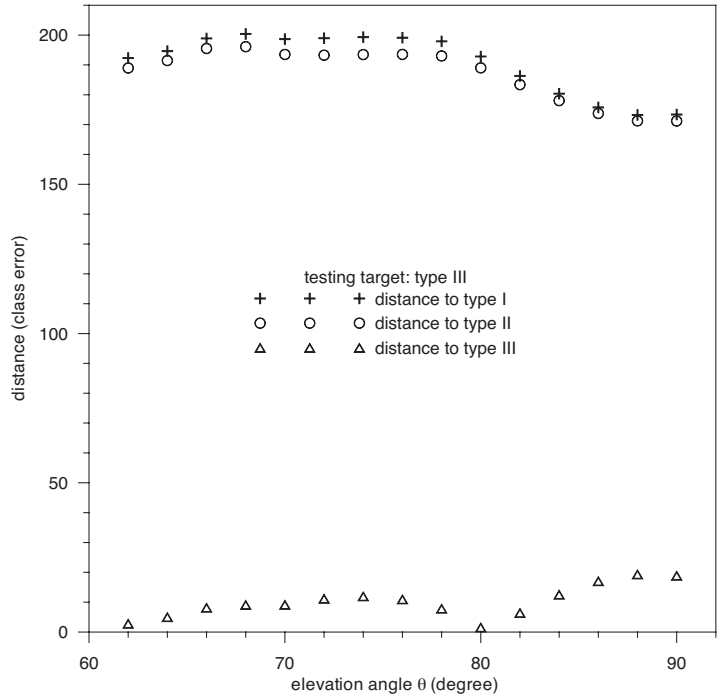

Figure 6. The distance (class error) to feature centers for the three known classes of ship RCS at different elevation angles θ by using ship of type III as the testing target.

The average of successful recognition rate is 100% (=45/45) in the above simulation. In this study, the 181-dimensional RCS vectors are projected into a two-dimensional eigenspace and performing recognition in the eigenspace can still maintain high level of recognition rate. Figure 7 shows the average of successful recognition rate with respect to the number of principal components (M'). In general,

increasing the number of principal components will improve the recognition rate. However, this will increase the computation work. From Figure 7, it is found that two principal components are adequate to achieve high recognition rate in such a problem.

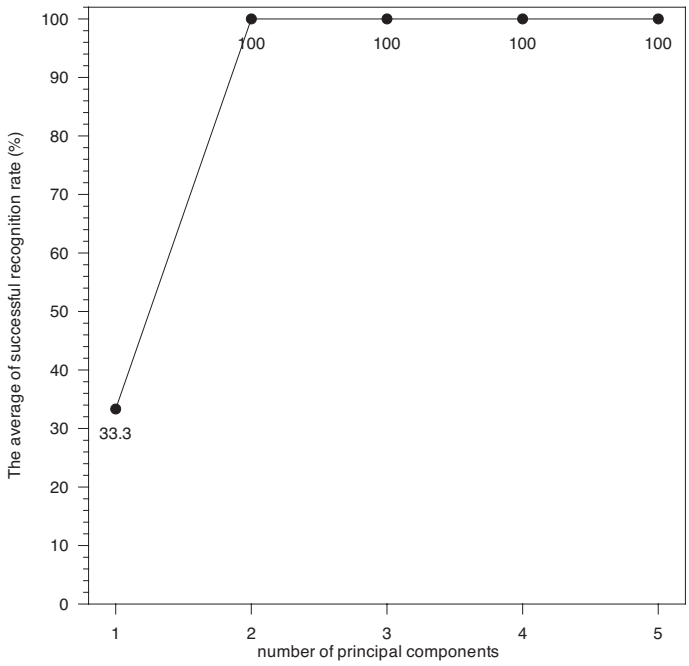

Figure 7. The average of successful recognition rate with respect to the number of principal components.

For investigating the effects of noise, we add to each RCS a quantity of independent random numbers having a Gaussian distribution with zero mean. The standard derivation of noise is normalized by the root-mean square value of the RCS. The standard derivations of applied noises include 10^{-4}, 10^{-3}, 10^{-2}, 10^{-1}, 2×10^{-1} and 4×10^{-1}. Figure 8 shows the mean of successful recognition rate with respect to noise levels. The recognition rates for the above noise levels are 100%, 100%, 100%, 95.3%, 91.8% and 79.6%, respectively. It shows that the effect of noise is tolerable to achieve recognition rate higher than 90% as noise levels are less than or equal to 2×10^{-1}.

The above numerical simulations (including the Ansoft HFSS software) are performed using personal computer with Pentium-3.0 CPU. The computer programs are coded using Fortran 90 in Absoft ProFortran 6.2.

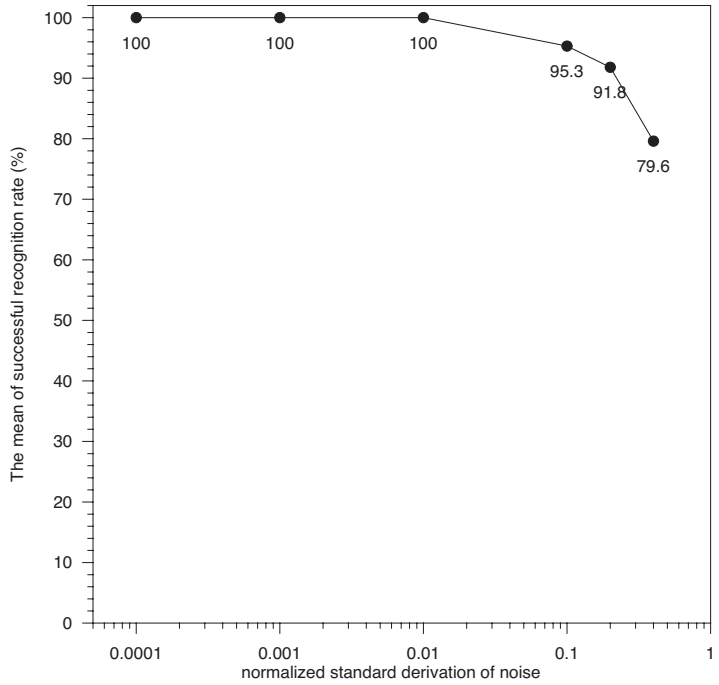

Figure 8. The mean of successful recognition rate with respect to noise levels.

4. CONCLUSION

In this paper, the angular-diversity radar recognition of ships is given by transformation based approaches with noise effects taken into consideration. Numerical simulation examples show that high recognition rate is achieved by using the proposed method. In addition, our recognition schemes can tolerate noise effects and still achieve high recognition rate. This is due to the inherent ability of noise suppression by the principal components analysis. The models of scatterers in this study are somewhat simple compared with the practical situation. However, this is not important because our main purpose is to illustrate that the transformation based approaches can reduce the dimensions of scattering data, tolerate noise effects and achieve high recognition rate in such angular-diversity arrangements. From physical points of view, the radar recognition from RCS is basically an approximate approach of inverse scattering [9–14]. Similar to the angular-diversity reconstruction of target shape in inverse scattering, the target ships are well classified by their angular-diversity RCS characteristics in this

study. With the use of transformation based approaches, the complex RCS data are projected into a small-dimensional eigenspace in the recognition procedures and high recognition rate can still be achieved under noise effects. This will make the radar recognition of ships very efficient and easy. Therefore, the work in this study can be applied to many other radar applications.

ACKNOWLEDGMENT

The work in this paper was supported by the National Science Council, Taiwan, under Grant NSC 95-2221-E-006-497. The authors would also like to express their sincere gratitude to National Center for High-performance Computing, Taiwan, for supporting the computing hardware and software.

REFERENCES

1. Hajduch, G., J. M. Le Caillec, and R. Garello, "Airborne high-resolution ISAR imaging of ship targets at sea," *IEEE Transactions on Aerospace and Electronic Systems*, Vol. 40, No. 1, 378–384, 2004.
2. Tello, M., C. Lopez-Martinez, and J. J. Mallorqui, "A novel algorithm for ship detection in SAR imagery based on the wavelet transform," *IEEE Geoscience and Remote Sensing Letters*, Vol. 2, No. 2, 201–205, 2005.
3. Farhat, N. H., "Microwave diversity imaging and automated target identification based on models of neural networks," *IEEE Proceedings*, Vol. 77, No. 5, 670–681, 1989.
4. Lee, K. C., *Polarization Effects on Bistatic Microwave Imaging of Perfectly Conducting Cylinders*, Master thesis, National Taiwan University, Taipei, Taiwan, 1991.
5. Moon, T. K. and W. C. Stirling, *Mathematical Methods and Algorithms for Signal Processing*, Prentice Hall, 2000.
6. Duda, R. O., P. E. Hart, and D. G. Stork, *Pattern Classification*, 2nd edition, John Wiley & Sons Inc., 2001.
7. Theodoridis, S. and K. Koutroumbas, *Pattern Recognition*, 2nd edition, Academic Press, Boston, 2003.
8. Ruck, G. T., D. E. Barrick, W. D. Stuart, and C. K. Krichbaum, *Radar Cross Section Handbook*, Vol. 1, Plenum, New York, 1970.
9. Bermani, E., A. Boni, A. Kerhet, and A. Massa, "Kernels evaluation of svm-based estimators for inverse scattering problems," *Progress In Electromagnetics Research*, PIER 53, 167–188, 2005.

10. Azaro, R., A. Casagranda, D. Franceschini, and A. Massa, "An innovative fuzzy-logic-based strategy for an effective exploitation of noisy inverse scattering data," *Progress In Electromagnetics Research*, PIER 54, 283–302, 2005.
11. Chiang, C. T. and B. K. Chung, "High resolution 3-D imaging," *Journal of Electromagnetic Waves and Applications*, Vol. 19, No. 9, 1267–1281, 2005.
12. Guo, B., Y. Wang, J. Li, P. Stoica, and R. Wu, "Microwave imaging via adaptive beamforming methods for breast cancer detection," *Journal of Electromagnetic Waves and Applications*, Vol. 20, No. 1, 53–63, 2006.
13. Semenov, S. Y., V. G. Posukh, A. E. Bulyshev, T. C. Williams, Y. E. Sizov, P. N. Repin, A. Souvorov, and A. Nazarov, "Microwave tomographic imaging of the heart in intact swine," *Journal of Electromagnetic Waves and Applications*, Vol. 20, No. 7, 873–890, 2006.
14. Chen, X., D. Liang, and K. Huang, "Microwave imaging 3-D buried objects using parallel genetic algorithm combined with FDTD technique," *Journal of Electromagnetic Waves and Applications*, Vol. 20, No. 13, 1761–1774, 2006.